The Association between Intraseasonal Oscillations and Tropical Storms in the Atlantic Basin

KINGTSE C. MO

Climate Prediction Center, NCEP/NWS/NOAA, Camp Springs, Maryland

(Manuscript received 4 October 1999, in final form 5 June 2000)

ABSTRACT

Tropical intraseasonal variations in the Pacific are related to the tropical storm activity in the Atlantic basin using outgoing longwave radiation anomalies (OLRAs) and circulation anomalies from the NCEP–NCAR reanalysis. Tropical storms are most likely to develop and maintain in the Atlantic, when enhanced convection associated with the tropical intraseasonal oscillations (TIOs) is located over the Indian Ocean and convection in the Pacific is suppressed. Tropical storm activity decreases when the TIO shifts to the opposite phase.

The dominant signal associated with the TIO is the Madden–Julian oscillation. The atmospheric response in the Tropics is a dipole pattern in the 200-hPa streamfunction anomalies just north of the equator. Positive OLRA propagates eastward from the Indian Ocean to the central Pacific. The dipole moves eastward in concert with OLRAs. When enhanced convection is located in the Indian Ocean and convection in the Pacific is suppressed, positive 200-hPa streamfunction anomalies as a part of the dipole extend from Central America to the central Atlantic. There are more upper-tropospheric easterly wind anomalies over the Caribbeans and the tropical Atlantic. The vertical wind shear decreases. These conditions are favorable for tropical storms to development and enhance. When the TIO shifts to the opposite phase with enhanced convection in the Pacific, the wind shear in the tropical Atlantic increases and the occurrence of tropical storms decreases.

1. Introduction

Atlantic seasonal tropical storm frequency exhibits large interannual variability. The occurrence of tropical storms can often be related to the large-scale atmospheric conditions. For example, Gray (1984a,b) related seasonal tropical cyclone activity to El Niño–Southern Oscillation (ENSO) and the stratospheric quasi-biennial oscillation. Bell and Chelliah (1998) discussed the influence of the Asian summer monsoons on tropical storms. The other contributing elements to the development and enhancement of tropical storms are local sea surface temperature anomalies in the Atlantic (Shapiro and Goldenberg 1998) and rainfall over the Sahel in Africa (Landsea and Gray 1992; Goldenberg and Shapiro 1996). All these factors have been used as predictors of hurricanes in the western Atlantic.

Many tropical storms start to develop in the area extending from Central America to the west coast of Africa over the tropical Atlantic from 5° to 20°N. This area has been labeled the ''main development region'' (MDR) by Goldenberg and Shapiro (1996). One of the critical elements controlling the development of hurricanes over the MDR is the tropospheric vertical wind shear defined as the difference between 200- and 850-hPa zonal winds. The vertical shear has negative influence on tropical cyclone genesis and intensification. The effect of shear has been attributed to ventilation (Gray 1968), and secondary circulation effect by Bender (1997) and vertical stability by DeMaria (1996). During warm ENSO events, there is an anomalous increase in upper-troposphere westerly winds over the Carribean Sea and the tropical Atlantic (Gray 1984a). Enhanced westerlies increase the vertical wind shear in the MDR. Strong wind shear in that area creates less favorable condition for cyclones to enhance and develop. The influence of the Asian monsoon and the quasi-biennial oscillation on tropical storm activity is also related to the changes in the vertical wind shear in the MDR. The vertical wind shear is not the only element influencing the tropical storms. Many tropical storms originate from African easterly waves (Pasch et al. 1998). The location and the strength of the easterly jet (Bell et al. 1999) also have an impact on rainfall over Africa and tropical storms in the Atlantic.

In addition to interannual variations, storm frequency is also modulated by the intraseasonal oscillations. Maloney and Hartmann (2000a,b) have documented the impact of the Madden–Julian oscillation (MJO) on hurricane activity over the eastern Pacific and the Gulf of

Corresponding author address: Kingtse Mo, Climate Prediction Center, NCEP/NWS/NOAA, 5200 Auth Rd., Camp Springs, MD 20746-4304.
E-mail: kmo@ncep.noaa.gov

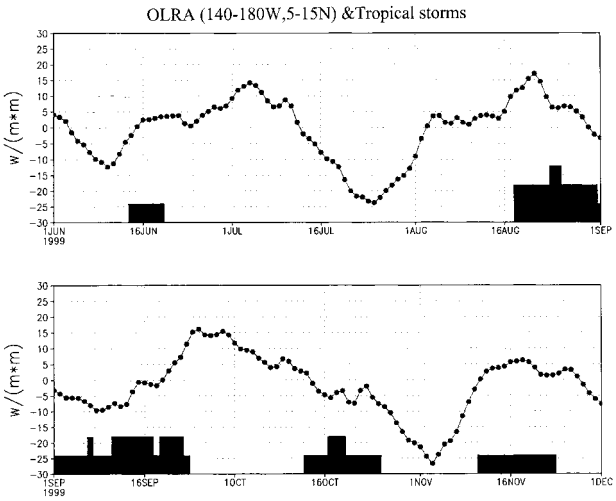

FIG. 1. The 5-day running mean (dark circles) of OLR averaged for the area (5°–15°N, 140°E–180°) for the period 1 Jun–1 Dec 1999 and tropical storm occurrence. The seasonal mean over this period was removed. The unit is 1 W m^{-2}. One dark step represents one tropical storm.

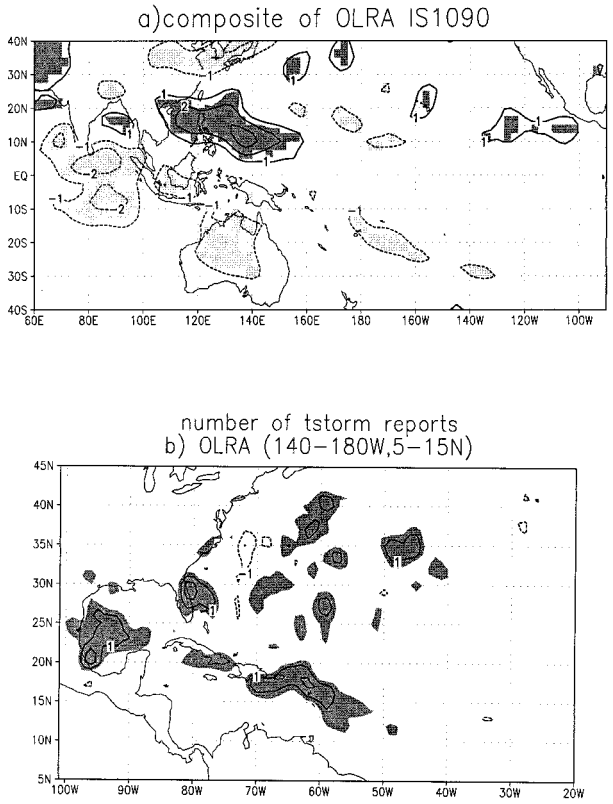

FIG. 2. (a) Composite of 10–90-day filtered OLRA for all tropical storm days. Contour interval is 2 W m^{-2}. Zero contours are omitted. Contours at −1 W m^{-2} and 1 W m^{-2} are added. Areas where positive (negative) values are statistically significant at the 95% level are shaded dark (light), and (b) difference of the total tropical storm reports between positive and negative cases based on the OLRA index. A nine-point smoother was applied before plotting. Contour interval is one report. Positive values are shaded.

Mexico. They reasoned that the MJO over the eastern Pacific influences the cyclonic low-level relative vorticity and the vertical wind shear. These factors in turn regulate the hurricane activity. Over the Atlantic, statistically significant lagged correlations are found between the monthly mean winds and monthly tropical storm frequency in the Atlantic basin (Shapiro 1987). He emphasized prediction and examined atmospheric conditions associated with month to month variability of tropical storm formation. The month to month variation of tropical storms was also evident during the 1999 season. Figure 1 displays the outgoing longwave radiation (OLR) averaged over the area (5°–15°N, 140°E–180°W) in the Pacific, with the seasonal mean removed, and the occurrence of tropical storms (dark bars) for the 1999 hurricane season. There was one named tropical storm, Arlene, from 11 to 16 June 1999. No named storm formed in July and three named hurricanes (Bret, Cindy, and Dennis) occurred between 18 and 28 August. They were followed by three named storms (Floyd, Gert, and Harvey) in September. After a short break, two hurricanes (Irene and Jose) occurred in October. The last hurricane (Lenny) came in November. The standard deviation of OLR anomalies (OLRAs) for the season was 18 W m^{-2}. All tropical storms occurred when OLRAs were positive or small negative (above −18 W m^{-2}). The period between the OLRA minima or maxima was roughly about 30–50 days. This suggests that intraseasonal oscillations may play a role in regulating tropical storm activity in the Atlantic.

In this paper, intraseasonal variations in the Pacific are related to the storm frequency in the Atlantic basin. Their relationships are established using OLRAs and circulation anomalies from the National Centers for Environmental Prediction–National Center for Atmospheric Research (NCEP–NCAR) reanalysis. The physical mechanisms are proposed and examined. Datasets used in this study are described in section 2. Evidence linking the tropical storm activity in the Atlantic and OLRAs in the Pacific is presented in section 3. Tropical storms are less likely to develop when convection in the Pacific is enhanced and convection in the Indian Ocean is suppressed. In section 4, this OLRA pattern is related to the leading mode in the intraseasonal band. The physical mechanisms responsible for such linkages are discussed in section 5. Conclusions and discussions are given in section 6.

2. Data

The positions and intensities of all Atlantic tropical cyclones are archived by the Hurricane Prediction Center in Miami. The Atlantic basin includes the tropical and subtropical regions north of the equator, the North Atlantic, the Caribbean Sea, and the Gulf of Mexico. These reports were archived four times daily for the

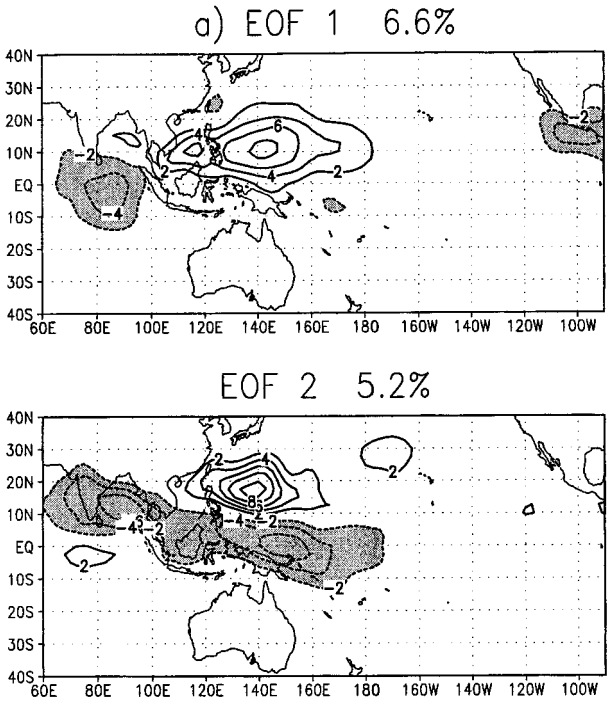

FIG. 3. (a) EOF1 and (b) EOF2 for the 10–90-day filtered OLRAs for Jul–Oct from 1979 to 1999. Contour interval is two nondimensional units. Zero contours are omitted, negative values are shaded.

period from 1886 to the present, but only data from 1974 to 1999 were used in this study because of the coverage of the OLR data. Here, tropical storms are defined as cyclones with the maximum sustained surface wind speed greater than 17 m s $^{-1}$ (Landsea and Gray 1992). Daily maps of tropical storms in the Atlantic can be derived from this dataset by counting reports of tropical storms at each grid point (1° resolution) within 24 h. When a tropical storm existed in the Atlanta basin during that day, that day was labeled as a tropical storm day. Daily averages of the National Oceanic and Atmospheric Administration satellite OLR data (Liebmann and Smith 1996) were used as a proxy for tropical convection. The OLR data cover the period from 1 June 1974 to 31 December 1999 with a 10-month gap in 1978. The global gridded analyses from the NCEP–NCAR reanalysis (Kalnay et al. 1996) were used to represent the atmospheric conditions. The data are on a 2.5° × 2.5° latitude–longitude grid and cover the period from 1 January 1974 to 31 December 1999. To obtain anomalies, the annual cycle was removed from daily data. To obtain the intraseasonal signal, data were filtered using the minimum bias window developed by Papoulis (1973) to retain periods in the range of 10–90 days.

3. Convection patterns in the Pacific and the Atlantic tropical storm activity

To examine the relationship between convection in the Pacific and the tropical storm activity in the Atlantic, the OLRA index was formed by averaging the 10–90-day filtered OLRA in the Pacific (5°–15°N, 140°E–180°W). A positive event starts when the OLRA index is above one standard deviation and that day is defined as the onset day. The event ends when the OLRA index drops below one standard deviation. The negative events can be selected the same way with a sign reversal. From the daily maps of tropical storms, one can calculate the total number of tropical storm reports at each grid point for all positive or negative events. Figure 2b shows the difference of the total number of tropical storm reports between positive and negative cases. The original map is too noisy. A nine-point smoother was applied to Fig. 2b before plotting. More tropical storms occur in the tropical Atlantic from the Gulf of Mexico to the Caribbean Sea, when the OLRA index is positive. There are more positive values over Florida and the eastern United States and negative values in the adjacent Atlantic. This suggests that more storms are landed over the eastern United States. Overall, there are 649 reports of tropical storms for the positive case and 443 reports for the negative case. There are 206 more reports for the positive category.

To test the statistical significance, the Monte Carlo test was performed. There are 650 days entering the composite for the positive case and 630 days for the negative case. A total of 1280 days were randomly selected. One can compute the mean difference between 640 pairs of randomly selected tropical storm maps. The process was then repeated 500 times so that there are 500 test cases. From 500 cases, one can derive the possibility at each grid point for more storms to occur. There is less than 5% probability for more storms to occur over Florida, the Gulf of Mexico, and the MDR randomly by chance. However, there is 10% probability for more storms to occur over the eastern United States by chance. To be statistically significant at the 95% level, the pattern correlation between Fig. 2b and any test case needs to be greater than 0.23. The pattern correlations between all test cases and Fig. 2b were calculated. There are only 2 cases out 500 where the pattern correlation is above 0.23. The correlation averaged over the collection of 500 independent cases is 0.01. One can also test the statistical significance of the total number of reports in the entire Atlantic basin regardless of the locations of the storms. From 500 random test cases, there is a 4% chance that the difference of tropical storm reports is greater than 206 reports. Therefore, Fig. 2b is statistically significant at the 95% level. Tropical storms are more likely to occur in the Atlantic when the OLRA index is positive.

If the above relationship is robust, then the composite of OLRAs in the Indian–Pacific sector for all tropical storm days should show suppressed convection in the central Pacific just above the equator. A composite of the 10–90-day filtered OLRA in the Indian–Pacific sector was obtained for days in which a tropical storm existed in the Atlantic basin (Fig. 2a). It shows positive

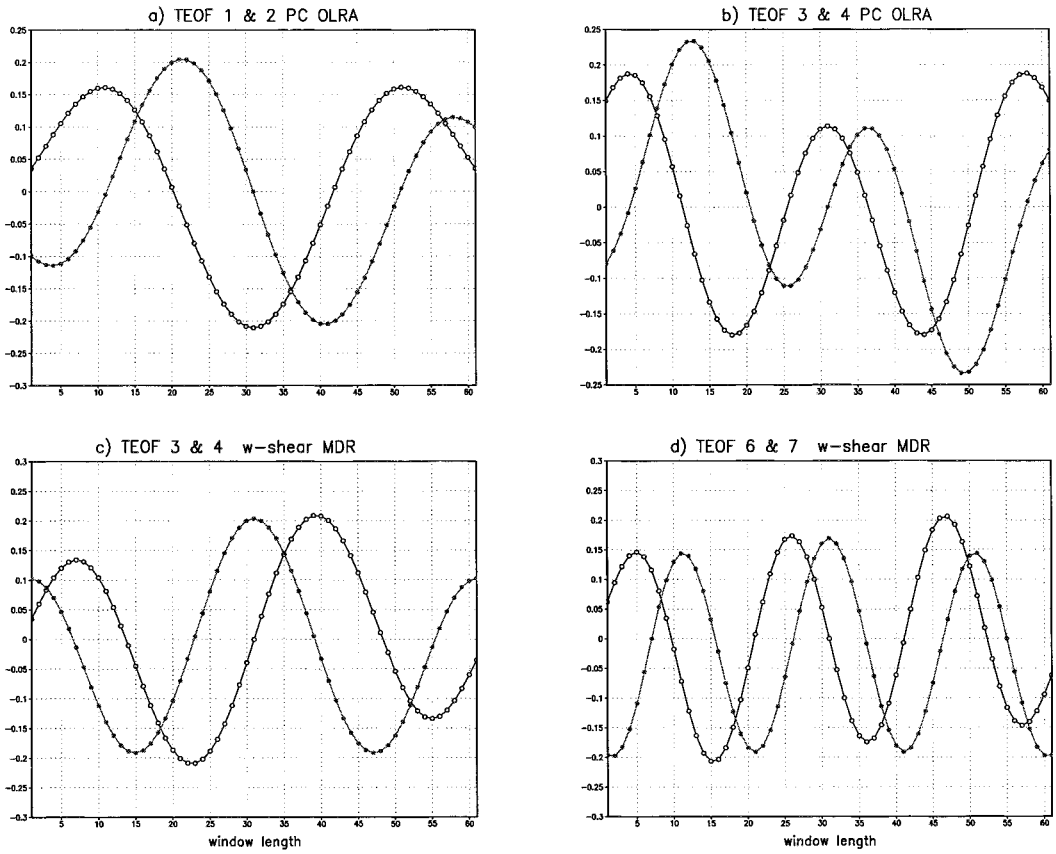

FIG. 4. (a) TEOF1 (open circles) and TEOF2 (dark circles) from SSA analysis for S-PC1. (b) Same as (a) but for T-EOF3 and T-EOF4. (c) T-EOF3 and T-EOF4 from SSA analysis for the wind shear index. (d) Same as (c) but for T-EOF6 and T-EOF7.

anomalies extending from 120°E to 160°W and negative OLRA extending from the Indian Ocean south of the equator to Australia. Figure 2a resembles the summer composite of OLRA associated with the MJO by Lau and Chan (1986).

Both the statistical significance of OLRA at each grid point and the field significance of the whole map (Fig. 2a) are tested by performing a Monte Carlo test. There are 740 maps entering the composite (Fig. 2a). One can randomly composite 740 maps of the 10–90-day filtered OLRA in the Indian–Pacific sector for August to October. The process was repeated 500 times. From 500 cases, one can test the statistical significance for OLRA at each grid point. The results show that the positive OLRAs in the western and the central Pacific are statistically significant at the 99% level and negative anomalies in the Indian Ocean from 10°S to 10°N are statistically significant at the 95% level. The negative anomalies over Indonesia are only significant at the 90% level, but negative anomalies near the South Pacific convergence zone (SPCZ) are statistically significant at the 95% level. Next, a field test is done. From 500 cases, one can calculate the percentage of grid points where the OLRAs at those grid points are statistically significant at the 95% level. The estimated percentage of statistically significant points is 27.3%. If one assumes 30–40 spatial degrees of freedom for the tropical Indian–Pacific sector, then the map (Fig. 2a) passes the field significance test of Livezey and Chen (1983, their Fig. 3). This indicates that the tropical storms in the Atlantic are more likely to occur when convection in the Pacific is suppressed and convection in the Indian Ocean is enhanced. Next, the convection pattern is related to the tropical intraseasonal oscillations (TIOs) in the Pacific.

4. The tropical intraseasonal oscillations

In this section, the leading spacial modes in the intraseasonal band are obtained by performing empirical orthogonal function (EOF) analysis for August–October. The principal components (PCs) associated with EOFs are then related to the Atlantic storm activity.

a. EOF analysis

EOF analysis was performed on the 10–90-day filtered OLRAs for July–October from 1979 to 1999 to avoid the gap in 1978. These months compose the major part of the hurricane season (Landsea 1993). To reduce the matrix size, the horizontal resolution was reduced

to 5° × 5°. Anomalies were not normalized but a latitudinal cosine weighting factor was used in computing the covariance matrix. The horizontal domain includes the Indian Ocean and the Pacific Ocean, where the TIO signal is strong. The first two EOFs (Fig. 3) explain 6.6% and 5.2% of the variance in the intraseasonal (10–90 day) band, respectively.

The first two EOFs resemble the tropical OLRA patterns representing the MJO for June–August (Lau and Chan 1986). EOF1 shows positive loadings extending from the western Pacific to the central Pacific. Negative loadings are located in Central America and in the Indian Ocean due to the Walker circulation. The pattern resembles the OLRA composite (Fig. 2a) based on tropical storm days. The pattern correlation between them is 0.45, which is statistically significant at the 95% level. EOF2 has positive loadings centered at 15°N and negative anomalies extending southeastward from the Indian Ocean to the central Pacific. EOF2 is nearly in quadrature with EOF1.

The 10–90-day filtered OLRAs from 1 August 1974 to 30 October 1999 were projected onto EOFs to obtain S-PCs (PCs associated with the spatial EOF). The simultaneous correlation between S-PC1 and S-PC2 is zero by definition. The maximum correlation between S-PC1 and S-PC2 is 0.45 with S-PC1 leading S-PC2 by 8–10 days. The correlations and the near-quadrature relationship between two EOFs suggest that the leading oscillation is in the range of the MJO. This can be verified using singular spectrum analysis (SSA).

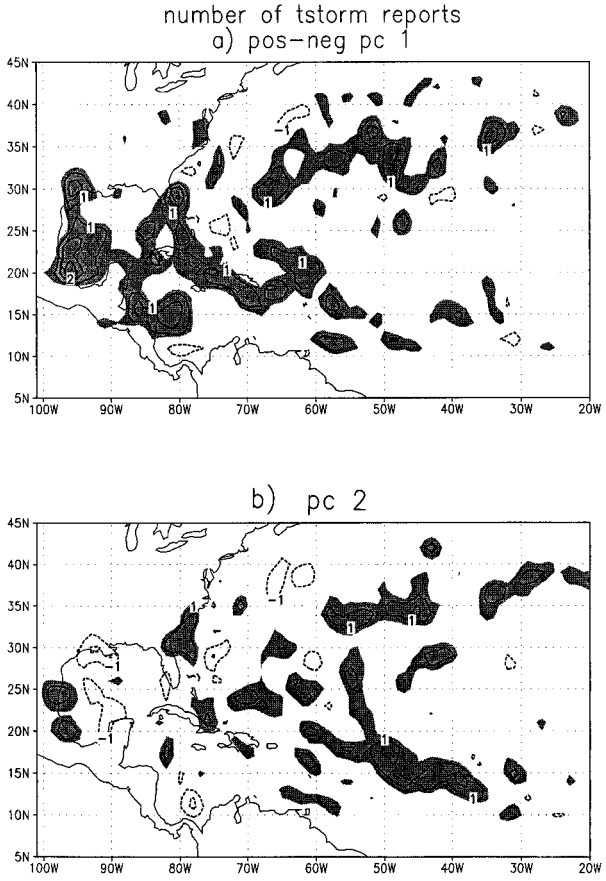

FIG. 5. Same as Fig. 2b but based on (a) S-PC1 and (b) S-PC2.

b. Leading oscillatory modes of S-PCs

S-PC1 and S-PC2 were subjected to SSA. SSA is a powerful tool for detecting oscillatory modes in a noisy time series (Vautard and Ghil 1989). It was used by Elsner et al. (1999) to examine fluctuations in the occurrence of hurricanes. Mo (1999) and Paegle et al. (2000) used SSA to determine the oscillatory modes modulating California and South America rainfall. Detailed procedures can be found in Vautard and Ghil (1989) and Paegle et al. (2000). Basically, it is an EOF analysis in the time domain. Oscillatory modes appear as a pair of T-EOFs (EOFs in the time domain) with degenerate eigenvalues and T-EOFs in quadrature with each other.

For both S-PC1 and S-PC2, there are two pairs of oscillatory modes. The first mode peaks at 40 days with T-EOFs in quadrature with each other (Fig. 4a) and explains about 46%–50% of the variance of a given S-PC in the 10–90-day band. This mode is in the range of the MJO and has the same properties as the MJO (Paegle et al. 2000). The second mode explains about 23% of the variance of a given S-PC and the estimated period is about 23–25 days (Fig. 4b)

c. Modulation of the tropical storm activity in the Atlantic

Figure 2 establishes the relationships between OLRA in the Pacific and the tropical storm activity in the Atlantic. The OLRA composite based on tropical storm days resembles the leading EOF (Fig. 4a) in the intraseasonal band for the hurricane season (August–October). The leading oscillatory mode is in the MJO range. If this relationship is robust, then one should be able to establish the relationships between S-PCs and the Atlantic storm activity.

The procedure used is the same as the one used to compute the difference of tropical storm reports based on the OLRA index (Fig. 2b). But now, composites were keyed to S-PCs. Positive and negative events can be selected based on S-PCs using the criterion of one standard deviation. Figure 5a displays the difference in the total number of tropical storm reports between positive and negative cases based on S-PC1 for August–October. Again, a nine-point smoother was applied to Fig. 5 before plotting. Figure 5a should be compared to the difference based on the OLRA index (Fig. 2b). There are similarities. Both show more tropical storms in the region from the Gulf of Mexico to the tropical Atlantic.

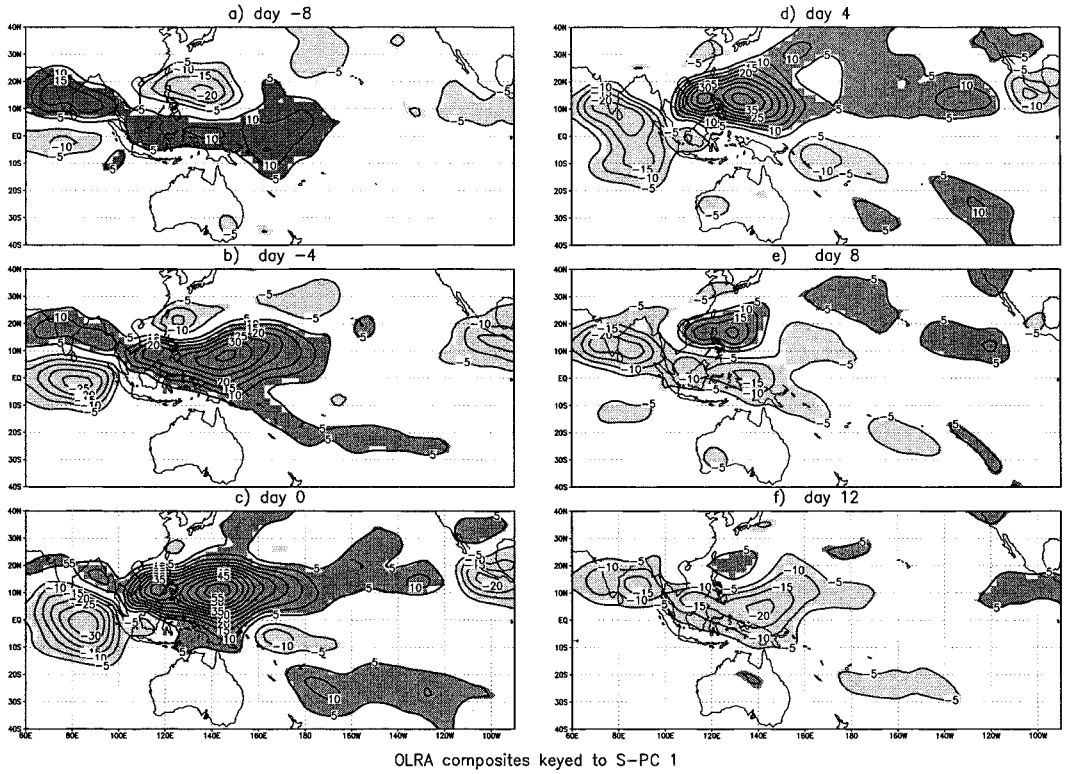

FIG. 6. Map sequences of OLRA composite difference between positive and negative category events keyed to the S-PC1 time series for (a) days -8, (b) -4, (c) 0, (d) 4, (e) 8, and (f) 12. Contour interval is 5 W m^{-2}. Zero contours are omitted. Areas where positive (negative) values are statistically significant at the 95% level are shaded dark (light).

Also, more storms landed in Florida. There are also some differences. For example, there is less storminess in Central America along 10°N for positive S-PC1 (Fig. 5a), but not for the positive OLRA index (Fig. 2a). All features discussed above are statistically significant at the 95% level by the Monte Carlo test.

There are a total of 766 reports of tropical storms for the positive S-PC1 case and 483 reports for the negative S-PC1 case. The difference of 283 reports is statistically significant at the 95% level determined by the Monte Carlo test. There are only 3 cases out 500 where the correlation between random samples and Fig. 5a is above 0.23.

The difference map keyed to S-PC2 (Fig. 5b) is very different from that of S-PC1 (Fig. 5a). There are more storms in the tropical Atlantic from 60° to 40°W, but there are fewer storms that landed in Florida and the Gulf states for the positive phase of S-PC2. The Monte Carlo test shows that negative values over the Gulf of Mexico and positive values from 60° to 40°W at 15°N are significant at the 95% level, while other features do not pass the test. The positive S-PC2 case has 58 more reports of tropical storms than the negative S-PC2 case. That difference is not statistically significant at the 95% level.

After establishing the statistical relationship between the tropical storm activity in the Atlantic and S-PC1, physical mechanisms to explain such linkages will be presented next.

5. Physical mechanisms

Lagged composites of the vertical wind shear anomaly field, OLRA, 200-hPa streamfunction, and 200-hPa zonal wind anomalies were computed for June–October from 20 days before to 20 days after onset based on the S-PC1 time series for positive and negative events. Composites for the positive and negative category events are similar with a sign reversal. Therefore, results are presented as the composite difference between positive and negative category events. The evolution of OLRAs keyed to S-PC1 is given in Fig. 6. At day −8, positive OLRAs extend southeastward from the Indian Ocean through the western Pacific to the date line with the maximum located in the Indian Ocean (15°N, 90°E). Negative OLRAs are located over the east coast of China and in the Indian Ocean just south of the equator. It resembles the negative phase of EOF2. As the time evolves, positive OLRAs propagate eastward to the central Pacific. At day 0, positive OLRAs extend east of the date line, while negative anomalies in the Indian Ocean strengthen. After day 0, the dipole with positive anomalies over the western Pacific and negative anomalies in the Indian Ocean shifts northward. At day 4,

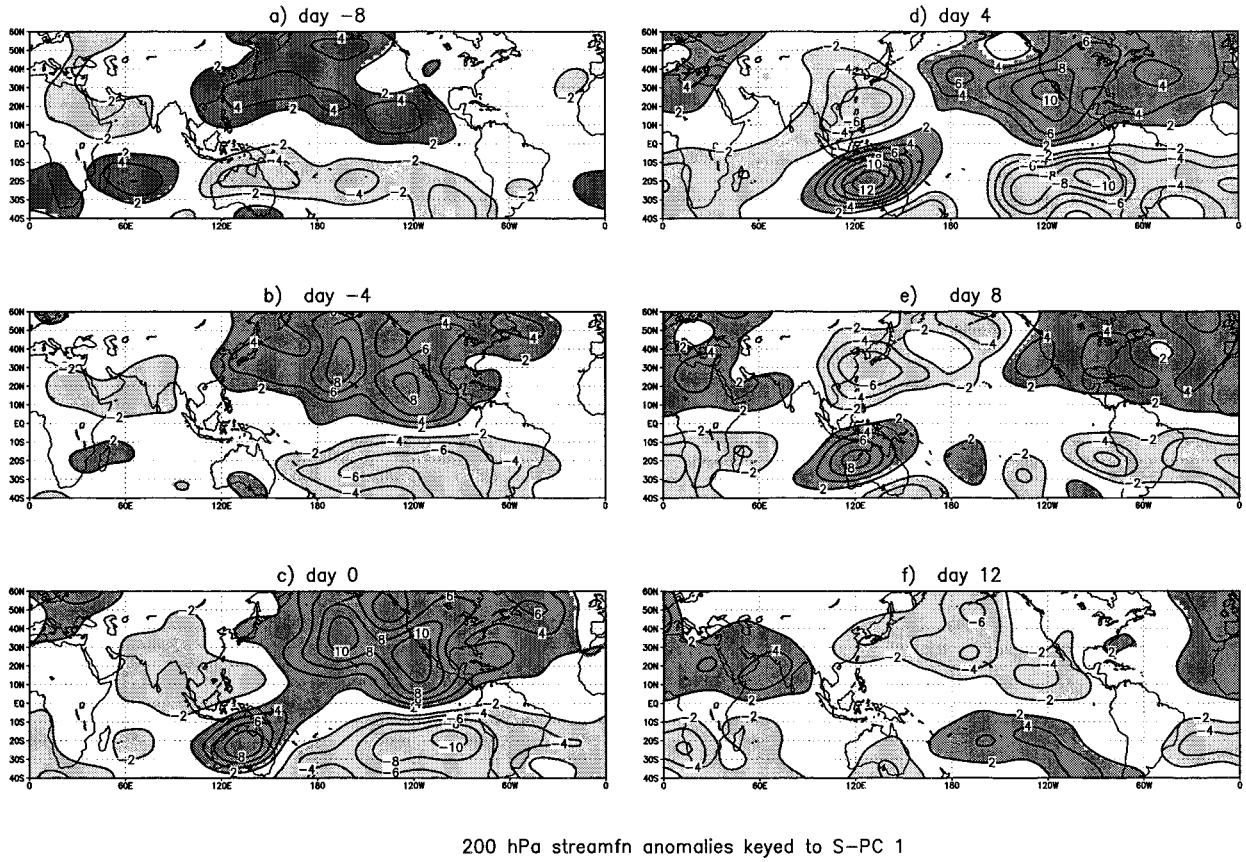

FIG. 7. Same as Fig. 6 but for 200-hPa streamfunction anomalies. Contour interval is 2×10^6 m^2 s^{-1}. Contours -1×10^6 m^2 s^{-1} and 1×10^6 m^2 s^{-1} are added.

negative OLRAs in the SPCZ area strengthen, while positive anomalies in the western Pacific are now centered at 15°N. The pattern resembles the OLRA composite based on tropical storm days (Fig. 2a). Negative anomalies over the Gulf of Mexico are consistent with more storm activity there (Fig. 5a). After day 8, positive OLRAs in the eastern Pacific diminish and negative OLRAs in the Indian Ocean strengthen. At day 12, the composite resembles that at day −8 with a sign reversal and the pattern is also similar to the positive phase of EOF2. Enhanced convection propagates eastward from the Indian Ocean to the central Pacific in 40 days. These are familiar features of the MJO (Knutson and Weickmann 1987). The evolution of S-PC1 resembles the evolution of the MJO for summer based on extended EOFs by Lau and Chan (1986), which is consistent with the SSA results that the MJO is the leading mode.

Figure 7 shows the 200-hPa streamfunction differences between positive and negative category events based on the S-PC1 time series. At day −8, the 200-hPa streamfunction composite (Fig. 7a) shows a dipole in the Pacific straddling the equator with positive anomalies north of the equator and negative anomalies south of the equator. There is another north–south dipole with a sign reversal located in the Indian Ocean. Positive anomalies in the Pacific and negative anomalies in the Indian sector centered at 10°N form an a east–west dipole. When positive OLRAs (suppressed convection) propagate eastward, the east–west dipole moves eastward in concert. Composites here resemble the composites based on the MJO for the extended summer season by Knutson and Weickmann (1987).

After day 0, positive 200-hPa streamfunction anomalies cover the tropical Atlantic from Central America to Africa. This is consistent with an enhancement of easterly wind anomalies in the Caribbean Sea and the western Atlantic as indicated by the 200-hPa zonal wind anomaly composite difference based on S-PC1 (Fig. 8a). The vertical wind shear in the MDR decreases (Fig. 8b). These conditions are favorable for tropical storms to develop and maintain. This can be confirmed by the wind shear anomaly composite for all tropical storm days in which a tropical storm existed in the tropical Atlantic (Fig. 8c). Figure 8c resembles the composite difference of wind shear anomalies keyed to S-PC1 (Fig. 8b). Both show that negative anomalies extend from the eastern Pacific to about 30°W with a minimum over the Carribean Islands. Anomalies are weak near the Africa continent. Low wind shear (negative wind shear anom-

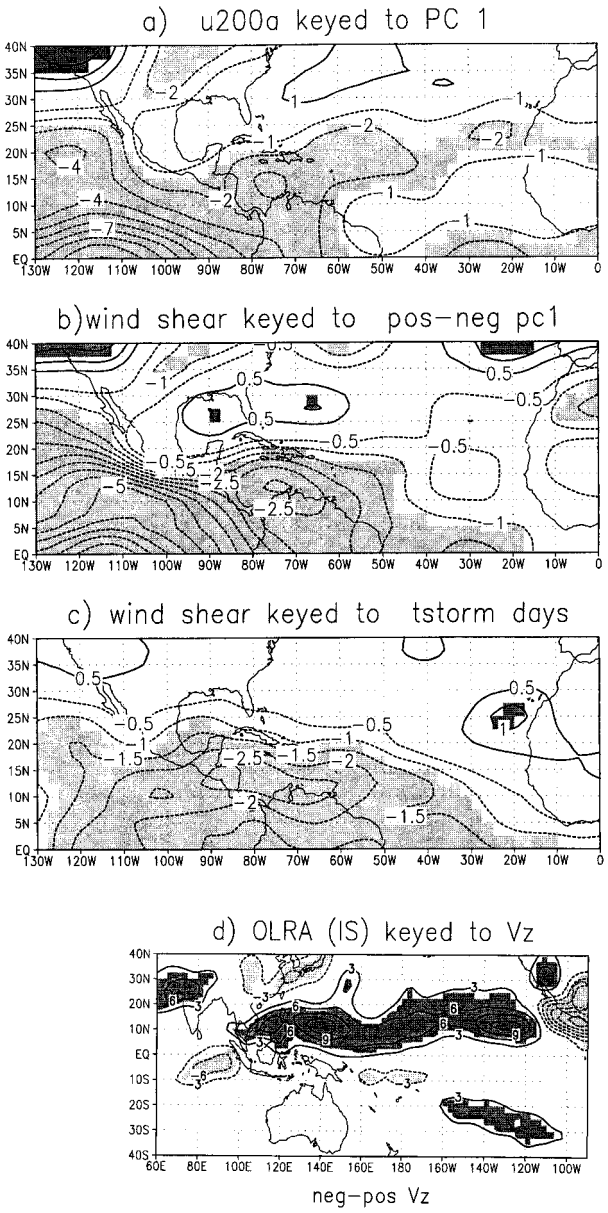

FIG. 8. (a) Composite difference of 200-hPa zonal wind anomalies between positive and negative category events for day 0 keyed to the S-PC1 time series. Contour interval is 1 m s^{-1}. Areas where positive (negative) values are statistically significant at the 95% level are shaded dark (light). (b) Same as (a) but for the vertical wind shear difference. Contour interval is 0.5 m s^{-1}. (c) Same as (b) but for composite of all tropical storm days. (d) Composite of 10–90-day filtered OLRA between negative and positive wind shear events. Contour interval is 3 W m^{-2}.

aly) in the tropical Atlantic favors the development of tropical storms.

Results in the above two sections indicate that suppressed convection in the Pacific Ocean and enhanced convection over the Indian Ocean favor the tropical storm development. The main reason is that the atmospheric response to this convection pattern is low wind shear in the tropical Atlantic. If this reasoning is sound, the composite of OLRA based on wind shear anomalies over the MDR should show positive OLRAs in the Pacific.

The wind shear index was formed by averaging the wind shear anomalies in the tropical Atlantic over the MDR (5°–15°N, 30°–120°W). The wind shear index was filtered to concentrate on the intraseasonal band. The composite difference of the 10–90-day filtered OLRA between negative and positive events based on the wind shear index (Fig. 8d) shows positive anomalies extending from the western Pacific to the central Pacific north of the equator and negative anomalies in the Indian Ocean south of the equator. These anomalies are statistically significant at the 95% level based on the Monte Carlo test. These key features resemble the composite of OLRA based on tropical storm days (Fig. 2a) and the composite at day 4 keyed to S-PC1 (Fig. 6d). This reenforces the relationship between the wind shear anomalies over the MDR and the convection pattern in the Indian–Pacific sector. If the composite is based on unfiltered wind shear index, the pattern is the same, but positive anomalies over the Pacific are weaker.

Notice that at day 0, positive OLRAs in the central Pacific are accompanied by negative OLRAs over the eastern North Pacific (Fig. 6c). Maloney and Hartmann (2000a) found that more tropical storms occur in the eastern North Pacific in the MJO phase (their phase 2, Fig. 3a) with less rainfall over the central Pacific and more convection over the eastern Pacific. The wind shear composite corresponding to convection pattern at day 0 (Fig. 8b) shows negative anomalies in the eastern North Pacific and these anomalies are a direct response to the MJO there. The central and eastern Pacific linkages are based on the equatorial wave dynamics. Here the situation is different. OLRAs in the tropical Atlantic based on the MJO composites are weak (not shown). The influence of the TIO on tropical storms in the Atlantic may be indirect. The impact seems to come from the atmospheric conditions associated with convection during the extreme phases of the TIOs The changes in wind shear are responses to the forcing from the Pacific. This can be verified by showing that the MJO signal in the Atlantic is weak. The wind shear index does not have spectra similar to the S-PCs. SSA was performed on the 10–90-day filtered wind shear index. The first pair of oscillatory mode appears as T-EOF3 and T-EOF4 (Figs. 4c and 4d). Together they explain only 15.2% of the variance and they have a peak near 34 days, which is shorter than the 40-day peak in the S-PCs. The second pair of oscillatory modes appears as T-EOF6 and T-EOF7. They have a peak at 21 days and explain about 10% of the variance. The wind shear index has oscillatory modes in the range of 34 days and 20–25 days. They are weaker and have slightly shorter periods in comparison to these intraseasonal modes in the tropical Pacific. SSA analysis on the OLRA averaged over the tropical Atlantic gives similar results. This indicates

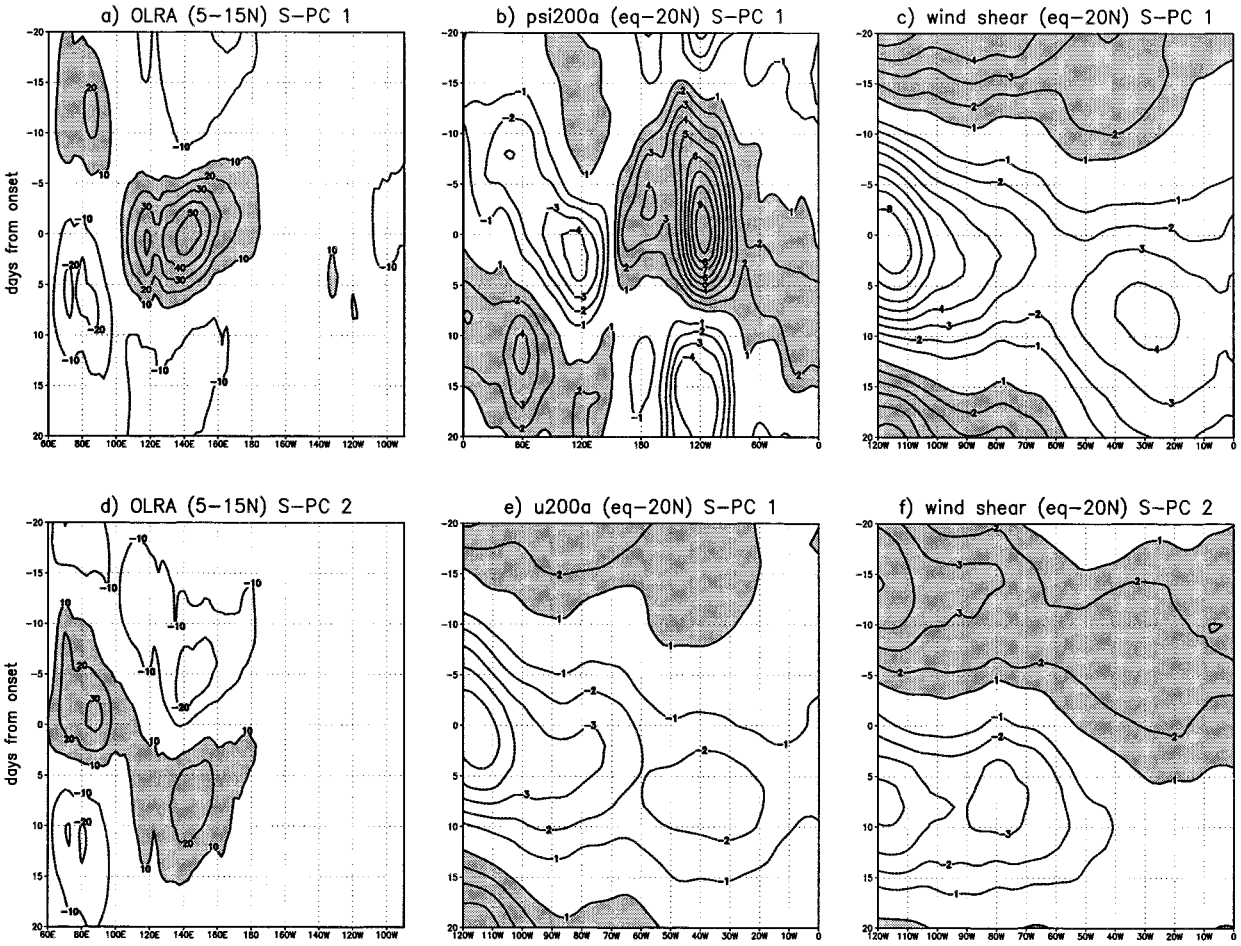

FIG. 9. (a) Time–longitude of cross section (Hovmöller diagram) of OLRA composite difference averaged from 5° to 15°N between positive and negative category events from 20 days before to 20 days after day 0 keyed to the S-PC1 time series. Contour interval is 10 W m^{-2}. Positive anomalies are shaded and zero contours are omitted. (b) Same as (a) but for 200-hPa streamfunction anomalies averaged from the equator to 20°N. Contour interval is 1×10^6 m^2 s^{-1}. (c) Same as (a) but for the vertical wind shear anomalies. Contour interval is 1 m s^{-1}. Positive values are shaded. (d) Same as (a) but keyed to S-PC2. (e) Same as (c) but for 200-hPa zonal wind anomalies. (f) Same as (c) but for S-PC2.

that the response of the wind shear in the MDR is remotely forced by the TIOs from the Pacific.

6. Conclusions

This paper has demonstrated that in addition to interannual and decadal variations, there is a modulation of tropical storm activity in the Atlantic by the TIO in the Pacific. Tropical storms are favored when convection is suppressed over the central Pacific and enhanced convection is located over the Indian Ocean. The situation reverses when the TIO shifts to the opposite phase.

The physical mechanisms responsible for the linkages between the TIOs in the Pacific and the Atlantic tropical storm activity are similar to the influence of ENSO on tropical storms in the Atlantic (Gray 1984). Figure 9 provides the summary. The time–longitude cross section of composite difference for OLRA just north of the equator between the positive and negative S-PC1 events from 20 days before and 20 days after day 0 is given in Fig. 9a. It shows that positive OLRAs (suppressed convection) shift from the Indian Ocean to the Pacific. There are both standing and propagating components. The period is about 40 days in the range of the MJO.

The response to the TIO revealed by the 200-hPa streamfunction is an east–west dipole just north of the equator. When positive OLRAs are located in the central Pacific (day -5 to day 5), the response in the 200-hPa streamfunction anomalies shows positive anomalies in the tropical Atlantic (Fig. 9b). The upper tropospheric easterly wind anomalies (negative wind anomalies) in that region are enhanced (Fig. 9e) and the vertical wind shear decreases (Fig. 9c). These conditions are favorable for tropical storms to develop. When enhanced convection propagates eastward, the dipole response in the 200-hPa streamfunction also moves eastward (Fig. 9b). The minimum of the wind shear anomalies in the equatorial Atlantic also shifts eastward from 120°W to the east

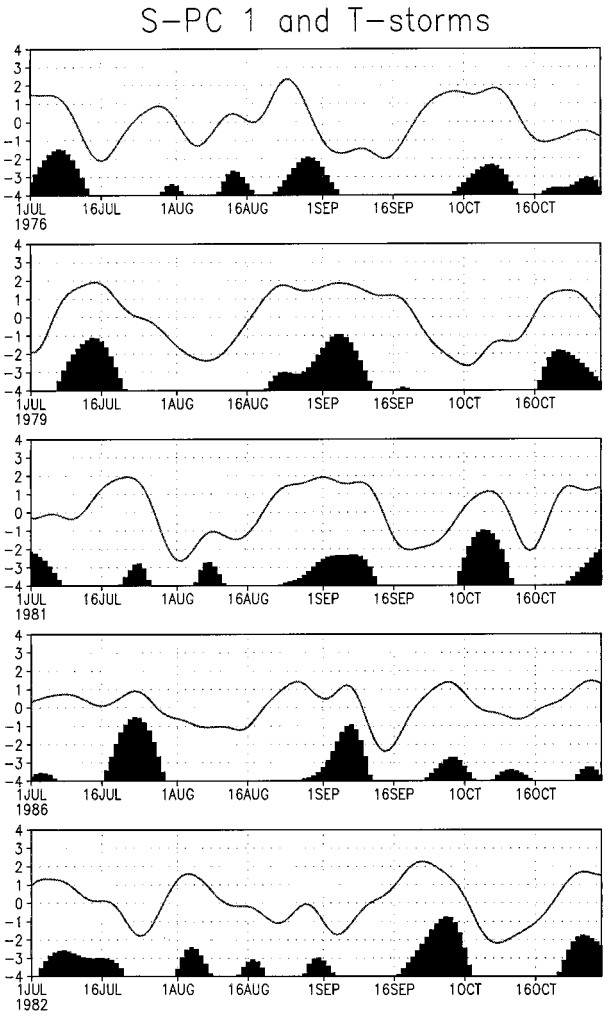

FIG. 10. Standardized S-PC1 together with tropical storm occurrence from 1 Jul to 30 Oct for (a) 1976, (b) 1979, (c) 1981, (d) 1986, and (e) 1982. One dark bar indicates one tropical storm in the Atlantic basin.

Atlantic near 30°W. When positive OLRAs move out of the central Pacific, they reappear from the Indian Ocean and the TIO reaches the other phase. The atmospheric responses also reverse. There are negative 200-hPa streamfunction anomalies in the MDR. The vertical wind shear is high and there are more westerlies in the MDR. This creates unfavorable conditions for tropical storms to enhance and develop.

These composites are based on the time series of S-PC1. One can form composites based on the time series of S-PC2. The composite differences of OLRA keyed to S-PC2 (Fig. 9d) lag the differences keyed to S-PC1 by about 8 days. Figures 9a and 9d show the same evolution of OLRAs. They are nearly in quadrature with each other. The corresponding responses in wind shear anomalies also (Fig. 9f) show similar evolution. The composites keyed to S-PC2 (Fig. 9f) lag composites keyed to S-PC1 (Fig. 9c) by 8–10 days. The evolution of the TIO remains the same and it is independent of the index used to form composites.

There are many factors influencing the tropical storm activity in the Atlantic. During warm ENSO years, enhanced convection in the Pacific suppresses the tropical storm development in the Atlantic by increasing the vertical wind shear in the MDR. In addition to ENSO, the hurricane frequency also shows strong decadal variability. This paper points out one additional factor, that is, the moderation of tropical storm activity by the TIO in the Pacific. There are seasons when the TIOs are strong. They can be identified by ranking the combined variance of S-PC1 and S-PC2. The five years having strong TIO were 1981, 1979, 1976, 1986, and 1982. Figure 10 plots S-PC1 for those years together with the occurrence of tropical storms in the Atlantic. There was less tropical storm activity when S-PC1 was below negative one standard deviation. This indicates that convection associated with the TIO may play a role in determining the tropical storm activity for those strong TIO years.

Acknowledgments. The author would like to thank the two reviewers. Their careful review and useful suggestions improved the paper.

REFERENCES

Bell, G. D., and M. Chelliah, 1998: The Africa easterly jet and its link to Atlantic basin cyclone activity and the global monsoon system. *Proc. 23th Annual Climate Diagnostics and Prediction Workshop*, Miami, FL, Climate Prediction Center/NWS/NOAA, 215–222.

——, M. S. Halpert, C. F. Ropelewski, V. Kousky, A. V. Douglas, R. C. Schnell, and M. Gelman, 1999: Climate assessment for 1998. *Bull Amer. Meteor. Soc.,* **80,** S1–S48.

Bender, M. A., 1997: The effect of relative flow on the asymmetric structure in the interior of hurricanes. *J. Atmos. Sci.,* **54,** 703–724.

DeMaria, M., 1996: The effect of vertical shear on tropical cyclone intensity change. *J. Atmos. Sci.,* **53,** 2076–2087.

Elsner, J. B., A. B. Kara, and M. A. Owens, 1999: Fluctuations in North Atlantic hurricane frequency. *J. Climate,* **12,** 427–437.

Goldenberg, S. B., and L. J. Shapiro, 1996: Physical mechanisms for the association of El Niño and west Africa rainfall with Atlantic major hurricane activity. *J. Climate,* **9,** 1169–1187.

Gray, W. M., 1968: Global view of the origin of tropical disturbances and storms. *Mon. Wea. Rev.,* **96,** 669–700.

——, 1984a: Atlantic seasonal hurricane frequency. Part I: El Niño and 30 mb quasi-biennial oscillation influences. *Mon. Wea. Rev.,* **112,** 1649–1668.

——, 1984b: Atlantic seasonal hurricane frequency. Part II: Forecasting its variability. *Mon. Wea. Rev.,* **112,** 1669–1683.

Kalnay, E., and Coauthors 1996: The NCEP/NCAR 40-Year Reanalysis Project. *Bull. Amer. Meteor. Soc.,* **77,** 437–471.

Knutson, T. R., and K. M. Weickmann, 1987: 30–60-day atmospheric oscillations: Composite life cycle of convection and circulation anomalies. *Mon. Wea. Rev.,* **115,** 1407–1435.

Landsea, C. W., 1993: A climatology of intense (or major) Atlantic hurricanes. *Mon. Wea. Rev.,* **121,** 1703–1713.

——, and W. M. Gray, 1992: The strong association between western Sahelian monsoon rainfall and intense Atlantic hurricanes. *J. Climate,* **5,** 435–452.

Lau, M. K., and P. H. Chan, 1986: Aspects of the 40–50-day oscil-

lation during the Northern Hemisphere summer as inferred from outgoing longwave radiation. *Mon. Wea. Rev.*, **114,** 1354–1367.
Liebmann, B., and C. A. Smith, 1996: Description of a complete (interpolated) outgoing longwave radiation dataset. *Bull. Amer. Meteor. Soc.*, **77,** 1275–1277.
Livezey, R. E., and W. Y. Chen, 1983: Statistical field significance and the determination by Monte Carlo techniques. *Mon. Wea. Rev.*, **111,** 46–59.
Maloney, E. D., and D. L. Hartmann, 2000a: Modulation of eastern North Pacific hurricanes by the Madden–Julian oscillation. *J. Climate*, **13,** 1451–1460.
——, and ——, 2000b: Modulation of hurricane activity in the Gulf of Mexico by the Madden–Julian oscillation. *Science*, **287,** 2002–2004.
Mo, K. C., 1999: Alternating wet and dry episodes over California and intraseasonal oscillations. *Mon. Wea. Rev.*, **127,** 2759–2776.
Paegle, J. N., L. A. Byerle, and K. C. Mo, 2000: Intraseasonal modulations of South American summer precipitation. *Mon. Wea. Rev.*, **128,** 837–850.
Papoulis, A., 1973: Minimum bias windows for high resolution spectral estimates. *IEEE Trans. Info. Theory*, **19,** 9–12.
Pasch, R. J., L. A. Avila, and J. G. Jiing, 1998: Atlantic tropical systems of 1994 and 1995: A comparion of a quiet season to a near record breaking one. *Mon. Wea. Rev.*, **126,** 1106–1123.
Shapiro, L. J., 1987: Month to month variability of the Atlantic tropical circulation and its relationship to tropical storm formation. *Mon. Wea. Rev.*, **115,** 2598–2614.
——, and S. B. Goldberg, 1998: Atlantic sea surface temperatures and tropical cyclone formation. *J. Climate*, **11,** 578–590.
Vautard, R., and M. Ghil, 1989: Singular spectrum analysis in nonlinear dynamics with applications to paleoclimatic time series. *Physica*, **35D,** 392–424.